

Kinematic Analysis of High Flow Unloading Device

Siyi LU¹

Storage & Loading Branch, China Coal Research Institute, Beijing 100013, China

Abstract. In order to realize the intelligent control of the unloading device and ensure the accurate loading of materials without intervention, it is particularly important to carry out the kinematic analysis of the edge of the unloading port of the unloading device, which is the basis for the control of the unloading device drive system. Firstly, this paper studies the two degree of freedom motion model of the hydraulic winch and the high flow unloading device driven by the hydraulic cylinder, derives the forward and inverse kinematics equations using the close-form method, and obtains the relationship between the length of the rope, the length of the cylinder and the spatial position of the edge of the unloading port. Secondly, the workspace of the device is analyzed by forward kinematics, and the reachable position of the edge of the unloading port is determined. Finally, the movement model of the unloading device is established by numerical method and visual model software, which verifies the correctness of the kinematics analysis. It lays a foundation for the following research on motion control of high flow unloading device.

Keywords. high flow unloading device; close-form method; forward and inverse kinematics; workspace

1. Introduction

The high flow unloading device is the loading execution part at the end of the rapid dosing station. Currently, the device is usually pulled by means of rope traction to achieve oscillation, and the height adjustment of the loading is achieved by the telescoping of hydraulic cylinders, so the unloading device has two degrees of freedom. In the past, some scholars have studied the structural form of the unloading device [1], the anti-impact design [2], the unloading flow control [3] and the simulation of the material flow process [4], but the kinematic part of the unloading device has not yet been analysed and studied. In the loading process, the motion of the unloading device determines when the car is ready to be loaded, the shape of the material loaded into the carriage and when it is lifted and waits until the next carriage reaches the loading position to start the next loading process, which requires the height of the carriage to be adjusted according to the height of the different carriages and the speed of the carriage travel, to ensure that the material does not overflow the carriage, does not spill and that the unloading device does not collide with the carriage. Therefore the motion process of the high flow unloading device needs to be analysed to explore the spatial position relationship between the rope length, cylinder length and the edge of the unloading port,

¹ Corresponding Author: Siyi LU, Storage & Loading Branch, China Coal Research Institute, e-mail: 534135979@qq.com

to ensure that the position of the edge of the unloading port is solvable, and thus complete the control of its position.

Kinematic analysis is the basis and prerequisite for device control and an important part of realising automatic and intelligent control. The existing widely used kinematic analysis methods are mainly the D-H method [5]-[7] and the closed vector method [8]-[12], with the D-H method mostly applied to series devices and the closed vector method mostly applied to parallel devices [13]-[18]. For the form of device studied in this paper, it is more intuitive and simple to use the closed vector method to analyse. In establishing the position equations of the device by the vector method, the main components of the device need to be represented by vectors and closed vector polygons are made, so firstly the coordinate system of the device is defined, secondly the kinematic equations are derived based on the structural form of the device and the principles of the vector method, and finally a trajectory within the range of motion of the device is given. The results are verified in joint space and working space.

2. Structure of the Device and Definition of the Coordinate System

The unloading device is mainly composed of oscillating section, telescopic section, hydraulic winches, hydraulic cylinders, wire rope, sensor, etc.

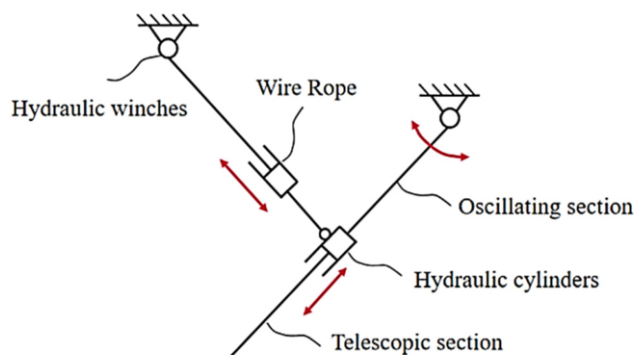


Figure 1. Organization diagram

A sketch of the device of the unloading device is shown in Figure 1, the specific action process is as follows: with the expansion and contraction of the wire rope, the rotation of the oscillating section around the hinge point can be realised, and the movement of the telescopic section along the axis direction can be realised by the expansion and contraction of the hydraulic cylinder.

According to the different dimensional parameters of each section, it can be divided into the following two cases and set the corresponding assumptions: when the unloading device swings, if the winch radius is relatively small then the position of the rope unloading point changes relatively little, it can be assumed that the position of the rope unloading point is fixed with the movement of the unloading device, ignoring the influence of the winch radius. If the winch radius is relatively large, the influence of the winch radius cannot be ignored, and the influence of the winch radius is considered in this paper.

Take the device structure shown in Figure 2 as an example, set the inertial coordinate system and inertial space fixed connection, device dynamic coordinate system with the unloading device body movement, the initial position of the two coordinate systems overlap, coordinate system origin are in the centre of oscillating, inertial coordinate system Y axis positive direction for the device oscillating home cylinder expansion direction, chute coordinate system (device dynamic coordinate system) Y axis positive direction for the cylinder expansion direction at any oscillating angle. This is shown in Figure 2. The rotation angle of the device dynamic coordinate system relative to the inertial coordinate system is defined as the oscillating angle α of the device, then the rotation transformation matrix between the device dynamic coordinate system and the inertial coordinate system is R .

$$R = \begin{bmatrix} \cos \alpha & -\sin \alpha & 0 \\ \sin \alpha & \cos \alpha & 0 \\ 0 & 0 & 1 \end{bmatrix}$$

The vectors in the dynamic coordinate system of the device represent: \vec{w}_p : spatial position vector between the rope and device connection point $\vec{w}_p = [w_{px}; w_{py}; 0]$; \vec{n}_p : spatial position vector between the cylinder and device connection point $\vec{n}_p = [n_{px}; n_{py}; 0]$; \vec{m}_p : spatial position vector between the piston rod and unloading device connection point and the lower edge of the unloading port $\vec{m}_p = [m_{px}; m_{py}; 0] = [-a + c; b; 0]$.

Vector representation in the inertial coordinate system: \vec{l}_0 : spatial position vector of the winch unloading point $\vec{l}_0 = [l_{0x}; l_{0y}; 0]$; \vec{l} : spatial position vector from the centre of rotation of the winch to the rope attachment point $\vec{l} = [l_x; l_y; 0]$; \vec{w} : spatial position vector of the rope attachment point with the unloading device $\vec{w} = R \cdot \vec{w}_p$; \vec{n} : spatial position vector of the cylinder connection point with the unloading device $\vec{n} = R \cdot \vec{n}_p$; \vec{s} : spatial position vector in the direction of expansion of the cylinder; \vec{m} : spatial position vector between the connection point of the piston rod with the unloading device and the lower edge of the unloading port $\vec{m} = R \cdot \vec{m}_p$; \vec{t} : spatial position vector of the lower edge of the unloading port $\vec{t} = [x_{down}; y_{down}; 0]$.

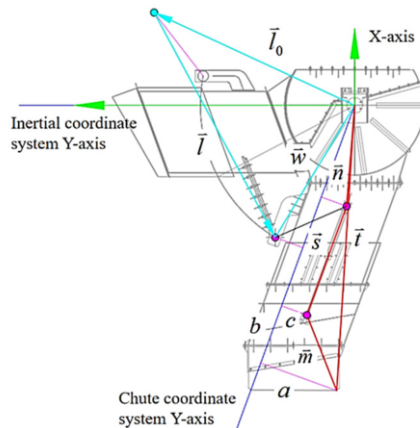


Figure 2. Schematic diagram of vector definition

Where a 、 b 、 c 、 n_{px} 、 n_{py} 、 w_{px} 、 w_{py} 、 l_{0x} 、 l_{0y} can be measured according to the actual unloading device structure, and in this paper, the above parameters are shown in Table 1, respectively.

Table 1. Structural parameters of unloading device

Parameters (mm)		
$a = 1524.2$	$b = 1148.46$	$c = 508.24$
$n_{px} = -508.24$	$n_{py} = 1844.68$	$w_{px} = 554.19$
$w_{py} = 2860.65$	$l_{0x} = 1754.8$	$l_{0y} = 3786.69$

3. Kinematic of the High Flow Unloading Devices

3.1. Inverse Kinematic of the Device

The inverse kinematics is to solve for the rope length and cylinder length given the spatial position coordinates of the edge of the unloading port, i.e. for the transformation from working space to joint space. The closed vector method is used for derivation, based on the structural model of the unloading device, the vectors associated with the motion process are selected to construct closed polygons, where one closed polygon is created for each of the oscillating and telescopic degrees of freedom, as shown in Figure 2.

The length of the rope is related to the vector of spatial positions of the rope and the connection point of the unloading device.

$$\vec{l}_0 + \vec{l} = \vec{w} \quad (1)$$

The spatial position vector along the lower edge of the unloading port can be represented by the cylinder direction vector as follows.

$$\vec{n} + \vec{s} + \vec{m} = \vec{t} \quad (2)$$

(1) Solve for the angle α of oscillation of the unloading device:

Assumptions, the angle between the Y-axis of the inertial coordinate system and the lower edge of the spatial position vector is α_1 , the angle between the Y-axis of the unloading device coordinate system and the spatial position vector along the lower edge is α_2 , $\alpha = \alpha_1 - \alpha_2$.

$$\alpha_1 = \begin{cases} \arctan \frac{|x_{down}|}{|y_{down}|}, y_{down} \geq 0 \\ \pi - \arctan \frac{|x_{down}|}{|y_{down}|}, y_{down} < 0 \end{cases}, \alpha_2 = \arctan \frac{a}{n_{py} + |\vec{s}| + b}$$

(2) Solve for the vector length $l_n = |\vec{l}|$ from the centre of rotation of the winch to the point where the rope is attached:

By shifting the term from Eq. (1), we get that,

$$\vec{l} = R \cdot \vec{w}_p - \vec{l}_0$$

Then, the vector length from the centre of rotation of the winch to the rope attachment point can be expressed as $|\vec{l}| = \sqrt{l_x^2 + l_y^2 + l_z^2}$.

(3) Consider the influence of the winch radius (this paper takes the winch radius as 200mm) and solve for the actual length l_s of the rope, which consists of two parts: the length of the vector from the rope out point to the rope attachment point $|\vec{l}_r|$, and the envelope length l_h . Using the Pythagorean theorem it can be solved that, $|\vec{l}_r| = \sqrt{|\vec{l}|^2 - R^2}$.

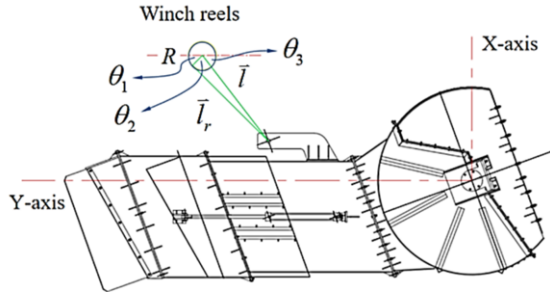


Figure 3. Geometric relation diagram of drawworks and rope outlet point

In order to more accurately drive the winch to turn a certain angle to change the rope length, the next calculation of the rope envelope length on the reel, as shown in Figure 3, the length of the envelope is noted as the arc length l_h corresponding to θ_1 .

$$l_h = R \cdot \theta_1 = R \cdot (\pi - \theta_2 - \theta_3) = R \cdot \left(\pi - \arccos \frac{R^2 + |\vec{l}| - |\vec{l}_r|}{2 \cdot R \cdot |\vec{l}|} - \arctan \frac{l_x}{l_y} \right)$$

$$l_s = |\vec{l}_r| + l_h$$

(4) Solve for cylinder length $s_n = |\vec{s}|$:

By shifting the term from Eq. (2), we get that,

$$\vec{s} = \vec{t} - R \cdot \vec{n}_p - R \cdot \vec{m}_p$$

Then, the cylinder length can be expressed as $|\vec{s}| = \sqrt{s_x^2 + s_y^2 + s_z^2}$.

3.2. Forward Kinematic of the Device

Forward kinematics is the spatial position coordinates of the known rope length l_s and cylinder length s_n to solve for the edge of the unloading port, i.e. the transformation from joint space to workspace.

Step 1: With a known rope length and a fixed centre of rotation of the winch and a fixed position of the rope attachment point relative to the unloading device, as shown in Figure 4, the oscillating angle α , i.e. $\alpha = \gamma - \delta + \beta$, can be solved for according to the geometric relationship.

Where γ is the angle between the outgoing rope point vector and the rope attachment point vector; δ is the angle between the outgoing rope point vector and the Y-axis of the inertial coordinate system; β is the angle between the rope attachment point vector and the Y-axis of the chute coordinate system.

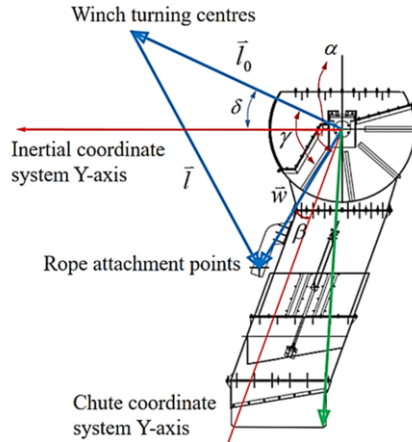


Figure 4. Schematic diagram of oscillating angle geometry

The geometric relationships shown in Figure 4 lead to γ , δ and β respectively as follows.

$$\cos\gamma = \frac{|\vec{l}_0|^2 + |\vec{w}|^2 - l_n^2}{2 \cdot |\vec{l}_0| \cdot |\vec{w}|} \tag{3}$$

$$\tan\delta = \frac{l_{ox}}{l_{oy}} \tag{4}$$

$$\tan\beta = \frac{w_{px}}{w_{py}} \tag{5}$$

The rotation matrix R can be solved by solving the angle from Eqs. (3)(4)(5).

Step 2: The spatial vector of the lower edge of the unloading device can be expressed under the coordinate system of the unloading device with its X-coordinate $-a$, its Y-coordinate $n_{py} + s_n + b$ and its Z-coordinate 0. The spatial vector of the lower edge of the unloading device can be expressed under the inertial coordinate system by transforming the rotation matrix.

$$t = R \cdot \begin{bmatrix} -a \\ n_{py} + s_n + b \\ 0 \end{bmatrix} = \begin{bmatrix} x_{down} \\ y_{down} \\ 0 \end{bmatrix}$$

4. Workspace Analysis

The two degrees of freedom of the unloading device are influenced by the mechanical structure of the device and have their own range of motion. Therefore, the oscillating

angle of the unloading device and the stroke of the cylinder are used as constraints to search for all the reachable spatial positions along the lower edge of the unloading port. The oscillating angle can be reflected by the length of the rope, so it is only necessary to change two variables, the rope length and the cylinder length, to obtain the spatial coordinates of the lower edge of the unloading port using the positive solution calculation. Based on the working space, the range of motion of the device can be derived, which can guide the trajectory planning of the control process, thus avoiding the phenomenon of the device colliding with the car gang.

According to the structural parameters of the unloading device in this paper, the safe working length of the rope fully extended and fully retracted ranges from 1516.25mm to 4829.5mm; the length of the cylinder when moving within the stroke ranges from 1190mm to 2190mm. The resulting working space is shown in Figure 5.

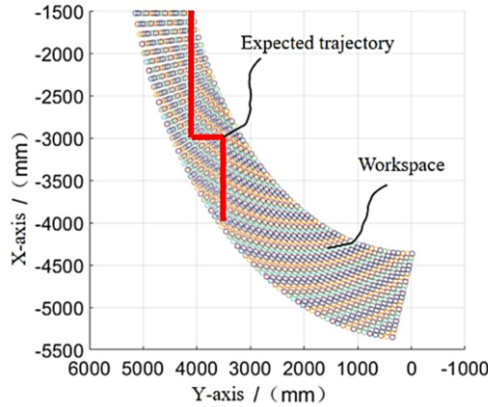


Figure 5. Working space at lower edge of unloading device

5. Simulation and Verification of Motion Relationships

5.1. Build a Visual Model

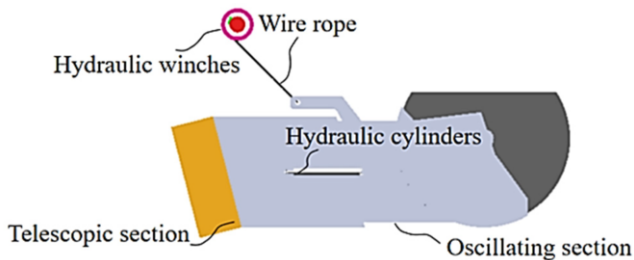


Figure 6. Three dimensional model of high flow unloading device

As shown in Figure 6, the visual 3D modelling software was used to model and analyse the motion of the unloading device. According to the actual motion of the device, motion subs and drives are added. The drive module outputs the rope and cylinder position information to observe the motion trajectory of the unloading device.

5.2. Validation of Forward and Inverse Kinematic Model Simulations

The kinematic inverse solution to the previous kinematics is modelled by taking the trajectory shown in Figure 5 over the ideal workspace range.

In practice, it is necessary to obtain the winch angle and cylinder expansion and contraction according to the rope length variation. Figure 7 and Figure 8 show the winch angle and cylinder extension length respectively, which are then imported into the drive interface of the visualisation model to drive the hydraulic winch and cylinder, thereby changing the model rope length and cylinder length to obtain the trajectory of the lower edge of the model.

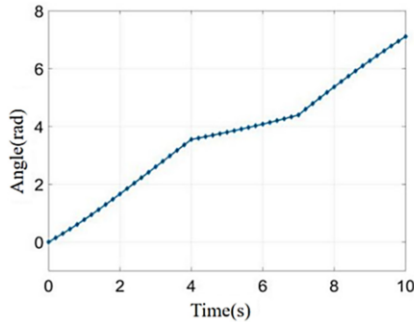


Figure 7. Winch angle

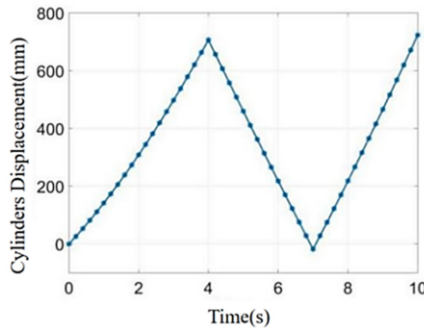


Figure 8. Hydraulic cylinder expansion and contraction

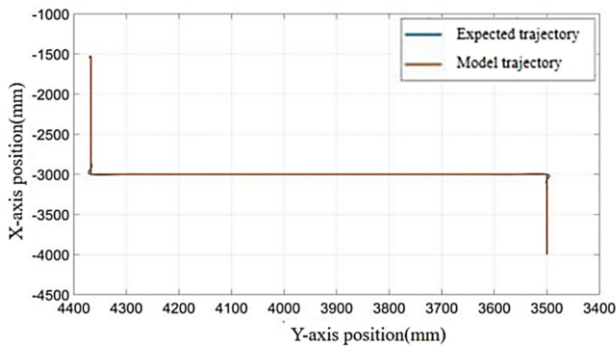


Figure 9. Comparison diagram of lower edge expectation and model output space position

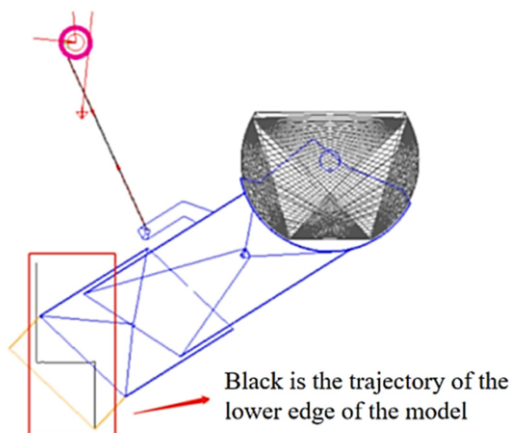


Figure 10. Track diagram of model simulation

As can be seen in Figure 9 and Figure 10, the trajectories output by the model coincide with the desired trajectories, so the X- and Y-directional motions satisfy the desired values.

6. Conclusion

Based on the results and discussions presented above, the conclusions are obtained as below:

(1) This paper simplifies the model of the high flow unloading device, determines the relationship between the rope length, cylinder length and the spatial position of the lower edge of the unloading port through coordinate transformation and closed vector method, and then can indirectly obtain the spatial position of the upper edge of the unloading port, and derives the kinematic equations of the device, i.e. on the one hand, the spatial position of the lower edge of the unloading port can be found by knowing the rope length and cylinder length; On the other hand, the spatial position of the lower edge of the unloading port can be found by knowing the spatial position of the lower edge of the unloading port. On the other hand, the length of the rope and the length of the cylinder can be found by knowing the spatial position of the lower edge of the unloading port.

(2) To guide the planning of the trajectory of the unloading device, the working space of the unloading device is analysed by numerical simulation, and the accessible position of the edge of the unloading port is determined more intuitively. It is a new solution for determining the end position of the unloading port, which is conducive to the intelligent implementation of the unloading device.

Acknowledgments

This work was financially supported by the Technology Innovation and Entrepreneurship Project of Tiandi Technology Co., Ltd (2022-2-TD-QN009).

References

- [1] Alexandru C. Design sensitivity analysis in the kinematics of the 4SS-axle guiding mechanism in Chebyshev configuration[J]. IOP Conference Series: Materials Science and Engineering, 2022, 1256(1).
- [2] Noufel Belkadi, Ferhat Djeddou, Lakhdar Smata, Abdenour Hosna, Abderazek Hammoudi. Optimization Study of the Effect of Manufacturing Tolerances on the Kinematic and Dynamic Performances of a Planar Mechanism[J]. SAE International Journal of Materials and Manufacturing, 2022, 16(1).
- [3] Ye Wei, Hu Lihuan, Li Qinchuan. Kinematic Analysis and Dimension Optimization of a New Reconfigurable Parallel Mechanism With 1R2T and 2R1T Operation Modes[J]. J. Mechanisms Robotics, 2022, 14(6).
- [4] Ren, Li, Ni, Mansheng. Kinematics analysis and scale synthesis of 3UPU parallel mechanism[J]. International Journal of System Assurance Engineering and Management, 2021.
- [5] Qi Zou, Dan Zhang, Shuo Zhang, Xueling Luo. Kinematic and dynamic analysis of a 3-DOF parallel mechanism[J]. International Journal of Mechanics and Materials in Design, 2021.
- [6] Manxin Wang, Qiusheng Chen, Haitao Liu, Tian Huang, Hutian Feng, Wenjie Tian. Evaluation of the Kinematic Performance of a 3- R RS Parallel Mechanism[J]. Robotica, 2020, 39(4).
- [7] S. Shankar Ganesh, A.B. Koteswara Rao. Kinematic and Dynamic Optimization of a 2-DOF Parallel Kinematic Mechanism[J]. Procedia Computer Science, 2018, 133.
- [8] Chawla Ishan, et al. Inverse and Forward Kineto-Static Solution of a Large-Scale Cable-Driven Parallel Robot using Neural Networks[J]. Mechanism and Machine Theory, 179.
- [9] Mobility Analysis of Parallel Mechanisms Using Screw Theory[J]. Journal of Machinery Manufacture and Reliability, 51(7): 591-600.
- [10] Inverse and Forward Kineto-Static Solution of a Large-Scale Cable-Driven Parallel Robot using Neural Networks[J]. Mechanism and Machine Theory, 179.
- [11] Kinematics Analysis and Singularity Avoidance of a Parallel Mechanism with Kinematic Redundancy[J]. Chinese Journal of Mechanical Engineering, 35(1).
- [12] Design and kinematic analysis of new multi-mode mobile parallel mechanism with deployable platform[J]. The Industrial Robot, 49(5): 885-902.
- [13] Forward Kinematics for Suspended Under-Actuated Cable-Driven Parallel Robots With Elastic Cables: A Neural Network Approach[J]. J. Mechanisms Robotics, 14(4).
- [14] Kinematics analysis and scale synthesis of 3UPU parallel mechanism[J]. International Journal of System Assurance Engineering and Management(prepublish): 1-9.
- [15] Design Optimization of 3-DOF Redundant Planar Parallel Kinematic Mechanism Based Finishing Cut Stage for Improving Surface Roughness of FDM 3D Printed Sculptures[J]. Mathematics, 9(9): 961-961.
- [16] The kinematics and design for isotropy of six-dof 3-CCC parallel mechanisms of general geometry and arbitrary actuation schemes[J]. Mechanism and Machine Theory, 178.
- [17] Closed-form solutions for the inverse kinematics of serial robots using conformal geometric algebra[J]. Mechanism and Machine Theory, 173.
- [18] Singularity analysis of a kinematically redundant (6+2)-DOF parallel mechanism for zero-torsion configurations[J]. Mechanism and Machine Theory, 170.